Zirconium Phosphinimide Complexes: Synthesis, Structure, and Deactivation Pathways in Ethylene Polymerization Catalysis

Nancy Yue, Emily Hollink, Fred Guérin, and Douglas W. Stephan*

School of Physical Sciences, Chemistry and Biochemistry, University of Windsor, Windsor, Ontario, Canada N9B 3P4

Received May 23, 2001

Zirconium phosphinimide complexes of the form $CpZr(NP\text{-}t\text{-}Bu_3)Cl_2$ (**1**) and $Cp^*Zr(NPR_3)Cl_2$ (R = *i*-Pr (**2**), *t*-Bu (**3**)) were readily prepared under ambient conditions via the reaction of $[CpZrCl_3]_n$ or Cp^*ZrCl_3 with the appropriate trialkylphosphinimide lithium salt (R_3PNLi). A series of derivatives were readily obtained via alkylation or arylation of the above dihalide precursors. These included $CpZr(NP\text{-}t\text{-}Bu_3)Me_2$ (**4**), $Cp^*Zr(NPR_3)Me_2$ (R = *i*-Pr (**5**), *t*-Bu (**6**)), $CpZr(NP\text{-}t\text{-}Bu_3)Ph_2$ (**7**), $Cp^*Zr(NPR_3)Ph_2$ (R = *i*-Pr (**8**), *t*-Bu (**9**)), $CpZr(NP\text{-}t\text{-}Bu_3)Bn_2$ (**10**), $CpZr(NP\text{-}t\text{-}Bu_3)(CH_2SiMe_3)_2$ (**11**), $Cp^*Zr(NPR_3)(allyl)_2$ (R = *i*-Pr (**12**), *t*-Bu **(13)**), $Cp^*Zr(NPR_3)(Cp)Cl$ (R = *i*-Pr (**14**), *t*-Bu (**15**)), and $Cp^*Zr(NPR_3)(CH_2C(CH_3)C(CH_3)CH_2)$ (R = *i*-Pr (**16**), *t*-Bu (**17**)). Reaction of **17** with the borane $B(C_6F_5)_3$ yielded the zwitterionic and cationic complexes $Cp^*Zr(NP\text{-}t\text{-}Bu_3)(CH_2C(CH_3)C(CH_3)CH_2B(C_6F_5)_3)$ (**18**) and $Cp^*Zr(NP\text{-}t\text{-}Bu_3)(THF)(CH_2C(CH_3)C(CH_3)CH_2B(C_6F_5)_3)$ (**19**). A number of the above compounds were screened for their potential as catalyst precursors in ethylene polymerization. In general, upon activation with methylaluminoxane, the resulting catalysts exhibit low activity. Efforts to understand the deactivation pathway for these zirconium catalysts involved investigating the interactions of catalyst precursors with activators. For example, reaction of **4** with the borane $B(C_6F_5)_3$ leads to aryl group transfer and formation of catalytically inactive $CpZr(NP\text{-}t\text{-}Bu_3)(C_6F_5)_2$ (**20**). Interactions with MAO were modeled via reaction with $AlMe_3$. The Zr clusters $(Cp^*Zr)_4(\mu\text{-}Cl)_5(Cl)(\mu\text{-}CH)_2$ (**21**) and $(Cp^*Zr)_5(\mu\text{-}Cl)_6(\mu\text{-}CH)_3$ (**22**) were two of the products that were characterized from these reactions. The isolation of **21** and **22** infers that aryl for methyl exchange, ligand abstraction, and C−H bond activation may be catalyst deactivation pathways.

Introduction

Industrial interest in early metal metallocene based single-site olefin polymerization catalysts has spurred studies of related systems for more than 20 years. More recently, systems that incorporate noncyclopentadienyl ancillary ligands have been the subject of intense study.[1] In our own efforts, we have uncovered several families of titanium-based ethylene polymerization precatalysts based on the steric analogy between phosphinimide ligands and cyclopentadienyl ligands.[2,3] In some cases, the resulting catalysts exhibit unprecedented activity.[2] The success of this approach appears to be the result of the steric demands that are remote from the metal center, making the immediate coordination sphere of the metal center accessible. While others have recently demonstrated that selected nonmetallocene derivatives of Zr do show good activity in olefin polymerization catalysis, the related systems that incorporate phosphinimide ligands have received only limited attention.[4−10] Thus, in this paper we report the synthesis and structure of a family of neutral CpZr− and Cp*Zr−phosphinimide complexes. The activation, utility in olefin polymerization, and deactivation pathways of corresponding zwitterionic and cationic Zr−phosphinimide catalysts are examined and considered in the light of previous work on Ti−phosphinimide systems.

Experimental Section

General Data. All preparations were done under an atmosphere of dry, O_2-free N_2 employing both Schlenk line techniques and Innovative Technologies, Braun, or Vacuum Atmospheres inert-atmosphere gloveboxes. Solvents were purified by employing Grubb type column systems manufac-

(1) Britovsek, G. J. P.; Gibson, V. C.; Wass, D. F. *Angew. Chem., Int. Ed.* **1999**, *38*, 428−447.
(2) Stephan, D. W.; Guérin, F.; Spence, R. E. v. H.; Koch, L.; Gao, X.; Brown, S. J.; Swabey, J. W.; Wang, Q.; Xu, W.; Zoricak, P.; Harrison, D. G. *Organometallics* **1999**, *18*, 2046−2048.
(3) Stephan, D. W.; Stewart, J. C.; Guérin, F.; Spence, R. E. v. H.; Xu, W.; Harrison, D. G. *Organometallics* **1999**, *18*, 1116−1118.
(4) Carraz, C.-A.; Stephan, D. W. *Organometallics* **2000**, *19*, 3791−3796.
(5) Guérin, F.; Stewart, J. C.; Beddie, C.; Stephan, D. W. *Organometallics* **2000**, *19*, 2994−3000.
(6) Guérin, F.; Stephan, D. W. *Angew. Chem., Int. Ed.* **2000**, *39*, 1298−1300.
(7) Kickham, J. E.; Guérin, F.; Stewart, J. C.; Stephan, D. W. *Angew. Chem., Int. Ed.*, **2000**, *39*, 3263−3266.
(8) Sung, R. C. W.; Courtenay, S.; McGarvey, B. R.; Stephan, D. W. *Inorg. Chem.*, **2000**, *39*, 2542−2546.
(9) Courtenay, S.; Stephan, D. W. *Organometallics* **2001**, *20*, 1442−1450.
(10) Kickham, J. E.; Guérin, F.; Stewart, J. C.; Urbanska, E.; Stephan, D. W. *Organometallics*, **2001**, *20*, 1175−1182.

10.1021/om010433q CCC: $20.00
Publication on Web 09/11/2001

tured by Innovative Technology.[11] All organic reagents were purified by conventional methods. Solvents used for the generation of zwitterionic species were further purified by distillation from Na/benzophenone. ^{1}H and ^{13}C{^{1}H} NMR spectra were recorded on Bruker Avance 300 and 500 spectrometers operating at 300 and 500 MHz, respectively. Trace amounts of protonated solvents were used as references, and chemical shifts are reported relative to $SiMe_4$. ^{31}P NMR, ^{11}B NMR, and ^{19}F NMR spectra were recorded on a Bruker Avance 300 and are referenced to 85% H_3PO_4, saturated $NaBH_4/H_2O$, and 80% $CFCl_3$ in $CDCl_3$, respectively. Guelph Chemical Laboratories performed combustion analyses. In some cases, particularly the alkyl derivatives, repeated attempts to obtain good elemental analyses were unsuccessful, despite the fact that X-ray-quality crystals of the respective compounds were sent. This reflects the limited stability and high sensitivity of these compounds. In these cases, ^{1}H NMR spectra have been deposited in the Supporting Information. The compounds $R_3PNSiMe_3$ and R_3PNLi were prepared via known methods.[12,13] $[CpZrCl_3]_n$, Cp^*ZrCl_3, and $AlMe_3$ were purchased from Aldrich and Strem Chemical Companies and used without further purification.

Synthesis of CpZr(NP-*t*-Bu$_3$)Cl$_2$ (1). Solid *t*-Bu_3PNLi (0.16 g, 0.72 mmol) was added in several portions over a 30 min period to a slurry of $[CpZrCl_3]_n$ (0.18 g, 0.72 mmol) in PhH (20 mL). The heterogeneous solution was stirred for 12 h at 25 °C, after which time it was filtered through Celite. Removal of the solvent in vacuo afforded a white crystalline solid (0.26 g, 81%). ^{1}H NMR (C_6D_6): δ 6.40 (s, 5H, C_5H_5), 1.10 (d, 27H, J_{P-H} = 12 Hz, $(CH_3)_3C$). ^{13}C{^{1}H} NMR (C_6D_6): δ 113.8, 41.0 (d, J_{P-C} = 28 Hz), 29.8. ^{31}P{^{1}H} NMR (C_6D_6): δ 40.7. Anal. Calcd for $C_{17}H_{32}Cl_2NPZr$: C, 46.26; H, 7.26; N, 3.17. Found: C, 46.21; H, 7.30; N, 3.16.

Synthesis of Cp*Zr(NPR$_3$)Cl$_2$ (R = *i*-Pr (2), *t*-Bu (3)). These compounds were prepared in a similar manner, and thus only one preparation is described in detail. To a slightly turbid yellow toluene solution (80 mL) of Cp^*ZrCl_3 (1.00 g, 3.00 mmol) was added a toluene solution (10 mL) of *i*-Pr_3PNLi (0.54 g, 3.00 mmol). The solution was stirred at room temperature overnight. The resulting solution was filtered. Removal of toluene under vacuum gave a yellow solid. **2**: yield 1.11 g (74%); ^{1}H NMR (C_6D_6) δ 2.16 (s, 15H, CH_3), 1.61 (m, 3H, CH, J_{H-H} = 7 Hz), 0.92 (dd, 18H, CH_3, J_{H-H} = 7 Hz, J_{P-H} = 12 Hz); ^{13}C{^{1}H} NMR (C_6D_6) δ 122.1, 26.3 (d, J_{P-C} = 59 Hz), 17.1, 12.3; ^{31}P{^{1}H} NMR (C_6D_6) δ 27.4. Anal. Calcd for $C_{19}H_{36}Cl_2NPZr$: C, 48.39; H, 7.69; N, 2.97. Found: C, 48.25; H, 8.83; N, 3.04. **3**: ^{1}H NMR (C_6D_6) δ 2.17 (s, 15H, $C_5(CH_3)_5$), 1.20 (d, 27H, J_{P-H} = 13 Hz, $(CH_3)_3C$); ^{13}C{^{1}H} NMR (C_6D_6) δ 121.9, 40.7 (d, J_{P-C} = 45 Hz), 29.6, 12.2; ^{31}P{^{1}H} NMR (C_6D_6) δ 42.2.

Synthesis of CpZr(NP-*t*-Bu$_3$)Me$_2$ (4), Cp*Zr(NPR$_3$)Me$_2$ (R = *i*-Pr (5), *t*-Bu (6)), CpZr(NP-*t*-Bu$_3$)Ph$_2$ (7), Cp*Zr(NPR$_3$)Ph$_2$ (R = *i*-Pr (8), *t*-Bu (9)), CpZr(NP-*t*-Bu$_3$)Bn$_2$ (10), CpZr(NP-*t*-Bu$_3$)(CH$_2$SiMe$_3$)$_2$ (11), and Cp*Zr(NPR$_3$)(allyl)$_2$ (R = *i*-Pr (12), *t*-Bu (13)). These compounds were prepared in a similar manner using the appropriate Grignard reagents and Zr precursor; thus, only one preparation is described in detail. A solution of MeMgBr (3.6 mmol) in Et_2O was added dropwise at room temperature to a slurry of **1** (0.32 g, 0.72 mmol) in the same solvent (30 mL). The heterogeneous mixture was stirred for 15 h, after which time the solvent was removed in vacuo. The product was extracted with hexanes (3 × 20 mL) and filtered through Celite. Removal of the solvent afforded a white solid (0.21 g, 72%). **4**: ^{1}H NMR (C_6D_6) δ 6.26 (s, 5H, C_5H_5), 1.16 (d, 27H, J_{P-H} = 13 Hz, $(CH_3)_3C$), 0.26 (s, 6H, $ZrCH_3$); ^{13}C{^{1}H} NMR (C_6D_6) δ 109.7, 40.3 (d, J_{P-C} = 47 Hz), 29.5, 28.1; ^{31}P{^{1}H} NMR (C_6D_6) δ 33.4. Anal. Calcd for $C_{19}H_{38}NPZr$: C, 56.67; H, 9.51; N, 3.48. Found: C, 53.59; H, 9.41; N, 3.18. **5**: yield 73 mg (80%); ^{1}H NMR (C_6D_6) δ 2.10 (s, 15H, CH_3), 1.64 (m, 3H, CH, J_{H-H} = 7 Hz), 0.98 (dd, 18H, CH_3, J_{H-H} = 7 Hz, J_{P-H} = 14 Hz), 0.08 (s, 6H, CH_3); ^{13}C{^{1}H} NMR (C_6D_6) δ 117.1, 31.3, 26.8 (d, J_{P-C} = 58 Hz), 17.5, 12.0; ^{31}P{^{1}H} NMR (C_6D_6) δ 22.5. **6**: yield 80%; ^{1}H NMR (C_6D_6) δ 2.09 (s, 15H, $C_5(CH_3)_5$), 1.24 (d, 27H, J_{P-H} = 12 Hz, $(CH_3)_3C$), 0.11 (s, 6H, $Zr-CH_3$); ^{13}C{^{1}H} NMR (C_6D_6) δ 116.6, 40.5 (d, J_{P-C} = 47 Hz), 31.8, 29.7, 11.6; ^{31}P{^{1}H} NMR (C_6D_6) δ 34.2 (s). **7**: light brown, crystalline solid (84%); ^{1}H NMR (C_6D_6) δ 7.95 (d, 4H, J_{H-H} = 7 Hz, C_6H_5 (*o*-H)), 7.31 (t, 4H, J_{H-H} = 7 Hz, C_6H_5 (*m*-H)), 7.21 (t, 2H, J_{H-H} = 7 Hz, C_6H_5 (*p*-H)), 6.38 (s, 5H, C_5H_5), 1.06 (d, 27H, J_{P-H} = 6 Hz, $(CH_3)_3C$); ^{13}C{^{1}H} NMR (C_6D_6) δ 183.9, 136.7, 126.9, 126.7, 111.5, 40.2 (d, J_{P-C} = 46 Hz), 23.0; ^{31}P{^{1}H} NMR (C_6D_6) δ 35.4 (s). **8**: yield 82%; ^{1}H NMR (C_6D_6) δ 7.94 (d, 4H, *o*-Ar, J_{H-H} = 7 Hz), 7.35 (t, 4H, *m*-Ar, J_{H-H} = 7 Hz), 7.23 (d, 2H, *p*-Ar, J_{H-H} = 7 Hz), 2.03 (s, 15H, Cp*), 1.60 (m, 3H, CH, J_{H-H} = 7 Hz), 0.85 (dd, 18H, CH_3, $|J_{H-H}|$ = 7 Hz, J_{H-H} = 14 Hz); ^{13}C{^{1}H} NMR (C_6D_6) δ 189.1, 137.0, 126.9, 126.8, 119.5, 26.4 (d, J_{P-C} = 57 Hz), 17.5, 12.6; ^{31}P{^{1}H} NMR (C_6D_6) δ 24.7. **9**: yield 79%, white solid; ^{1}H NMR (C_6D_6) δ 7.95 (d, 4H, *o*-Ar, J_{H-H} = 7 Hz), 7.34 (t, 4H, *m*-Ar, J_{H-H} = 7 Hz), 7.21 (d, 2H, *p*-Ar, J_{H-H} = 7 Hz), 1.98 (s, 15H, Cp*), 1.10 (d, 27H, CH_3, J_{H-H} = 12 Hz); ^{13}C{^{1}H} NMR (C_6D_6) δ 189.5, 136.8, 126.9, 126.7, 119.5, 40.7 (d, C, J_{P-C} = 47 Hz), 30.0, 12.7; ^{31}P{^{1}H} NMR (C_6D_6) δ 35.8. Anal. Calcd for $C_{34}H_{52}NPZr$: C, 68.40; H, 8.78; N, 2.35. Found: C, 68.50; H, 8.72; N, 2.39. **10**: light brown solid when washed with Et_2O (80%); ^{1}H NMR (C_6D_6) δ 7.22 (t, 4H, J_{H-H} = 8 Hz, C_6H_5 (*o*-H)), 7.03 (d, 4H, J_{H-H} = 7 Hz, C_6H_5 (*m*-H)), 6.93 (t, 2H, J_{H-H} = 9 Hz, C_6H_5 (*p*-H)), 5.95 (s, 5H, C_5H_5), 2.48, 2.03 (AB q, 4H, J_{H-H} = 10 Hz, $CH_2C_6H_5$), 1.09 (d, 27H, J_{P-H} = 13 Hz, $(CH_3)_3-C-$); ^{13}C{^{1}H} NMR (C_6D_6) δ 149.9, 130.0, 126.3, 120.7, 111.7, 56.5, 40.2 (d, J_{P-C} = 45 Hz), 29.5; ^{31}P{^{1}H} NMR (C_6D_6) δ 35.4. **11**: white solid (77%); ^{1}H NMR (C_6D_6) δ 6.35 (s, 5H, C_5H_5), 1.15 (d, 27H, J_{P-H} = 13 Hz, $(CH_3)_3C$), 0.34 (s, 18H, $CH_2Si(CH_3)_3$), 0.47, 0.07 (AB q, 4H, J_{H-H} = 11 Hz, $CH_2Si(CH_3)_3$); ^{13}C{^{1}H} NMR (C_6D_6) δ 109.5, 42.5, 40.4 (d, J_{P-C} = 47 Hz), 29.6, 4.3; ^{31}P{^{1}H} NMR (C_6D_6) 34.0. **12**: yield 71%; ^{1}H NMR (C_6D_6) δ 6.00 (quint, 2H, CH, J_{H-H} = 12 Hz), 3.23 (d, 4H, CH_2, J_{H-H} = 12 Hz), 1.88 (s, 15H, Cp*), 1.54 (m, 3H, CH, J_{H-H} = 7 Hz), 0.84 (dd, 18H, J_{H-H} = 7 Hz, J_{H-H} = 14 Hz); ^{13}C{^{1}H} NMR (C_6D_6) δ 143.4, 115.1, 73.4, 26.4 (d, J_{P-C} = 57 Hz), 17.6, 12.2; ^{31}P{^{1}H} NMR (C_6D_6) δ 21.3. **13**: yield 73%, white solid; ^{1}H NMR (C_6D_6) δ 6.04 (quint, 2H, CH, J_{H-H} = 12 Hz), 3.27 (d, 4H, CH_2, J_{H-H} = 12 Hz), 1.89 (s, 15H, Cp*). 1.12 (d, 27H, CH_3, $|J_{H-H}|$ = 18 Hz); ^{13}C{^{1}H} NMR (C_6D_6) δ 143.6, 115.1, 73.3, 41.1 (d, J_{P-C} = 46 Hz), 30.1, 12.2; ^{31}P{^{1}H} NMR (C_6D_6) δ 29.1.

Synthesis of Cp*Zr(NPR$_3$)(Cp)Cl (R = *i*-Pr (14), *t*-Bu (15)). Both compounds were prepared via similar routes; thus, only one representative procedure is described. To a yellow THF solution (5 mL) of **2** (100 mg, 0.21 mmol) was added a THF solution of (3 mL) NaCp·2THF (123 mg, 0.53 mmol). The solution was stirred at room temperature overnight. Removal of benzene under vacuum gave a yellow solid. The solid was extracted with 4 × 5 mL of hexane, followed by filtration and evaporation under vacuum. **14**: yield 57%, light yellow solid; ^{1}H NMR (C_6D_6) δ 6.13 (s, 5H, Cp), 1.99 (s, 15H, Cp*), 1.75 (m, 3H, CH, J_{H-H} = 7 Hz), 0.98 (dd, 18H, CH_3, J_{H-H} = 7 Hz, J_{P-H} = 14 Hz); ^{13}C{^{1}H} NMR (C_6D_6) δ 119.0, 111.7, 27.9 (d, CH, J_{P-C} = 57 Hz), 17.4, 12.5; ^{31}P{^{1}H} NMR (C_6D_6) δ 24.0. Anal. Calcd for $C_{24}H_{41}ClNPZr$: C, 57.51; H, 8.24; N, 2.79. Found: C, 57.76; H, 9.11; N, 2.91. **15**: yield 68%, light yellow solid; ^{1}H NMR (C_6D_6) δ 6.27 (s, 5H, Cp), 2.02 (s, 15H, Cp*), 1.28 (d, 27H, CH_3, J_{H-H} = 12 Hz); ^{13}C{^{1}H} NMR (C_6D_6) δ 119.9, 112.3, 41.2 (d, J_{P-C} = 46 Hz), 30.5, 12.9; ^{31}P{^{1}H} NMR (C_6D_6) δ 37.8.

Synthesis of Cp*Zr(NPR$_3$)(CH$_2$C(CH$_3$)C(CH$_3$)CH$_2$) (R = *i*-Pr (16), *t*-Bu (17)). These compounds were prepared in a similar manner, and thus a single preparation is detailed. To a yellow THF solution (5 mL) of **3** (100 mg, 0.19 mmol) was

(11) Pangborn, A. B.; Giardello, M. A.; Grubbs, R. H.; Rosen, R. K.; Timmers, F. J. *Organometallics* **1996**, *15*, 1518.
(12) Latham, I. A.; Leigh, G. J.; Huttner, G.; Jibril, I. *J. Chem. Soc. D* **1986**, 377−384.
(13) Rubenstahl, T.; Weller, F.; Harms, K.; Dehnicke, K. *Z. Anorg. Allg. Chem.* **1994**, *620*, 1741−1749.

added excess Mg (14 mg, 0.59 mmol). After 30 min of stirring, the solution mixture became deep blue, and 2,3-dimethyl-1,3-butadiene (16 mg, 0.19 mmol) was added. The resulting solution was stirred at room temperature overnight. Removal of THF under vacuum gave a dark green solid. Extraction with 4 × 5 mL of hexane and subsequent removal of the solvent gave 77 mg (75%) of orange solid product, **17**. **16**: yield 76%, orange solid; ^{1}H NMR (C_6D_6) δ 2.73 (d, 2H, CH_2, J_{H-H} = 9 Hz), 2.14 (s, 15H, Cp*), 2.10 (s, 6H, CH_3), 1.55 (m, 3H, CH, J_{H-H} = 7 Hz), 0.87 (dd, 18H, CH_3, J_{H-H} = 7 Hz, J_{P-H} = 14 Hz), −0.06 (d, 2H, CH_2, J_{H-H} = 9 Hz); ^{13}C{^{1}H} NMR (C_6D_6) δ 115.6, 112.2, 57.2, 28.0 (d, J_{P-C} = 57 Hz), 25.0, 17.9, 12.7; ^{31}P{^{1}H} NMR (C_6D_6) δ 19.1. Anal. Calcd for $C_{25}H_{46}NPZr$: C, 62.19; H, 9.60; N, 2.90. Found: C, 61.89; H, 9.40; N, 2.58. **17**: ^{1}H NMR (C_6D_6) δ 2.20 (s, 6H, CH_3), 2.17 (d, 2H, CH_2, J_{H-H} = 11 Hz), 2.12 (s, 15H, Cp*), 1.12 (d, 27H, CH_3, J_{P-H} = 12 Hz), 0.38 (d, 2H, CH_2, J_{H-H} = 11 Hz); ^{13}C{^{1}H} NMR (C_6D_6) δ 121.6, 115.8, 55.3, 40.0 (d, J_{P-C} = 48 Hz), 30.5, 25.6, 12.7; ^{31}P{^{1}H} NMR (C_6D_6) δ 33.2. Anal. Calcd for $C_{28}H_{52}NPZr$: C, 64.07; H, 9.98; N, 2.67. Found: C, 63.87; H, 9.67; N, 2.54.

Generation of Cp*Zr(NP-*t*-Bu$_3$)(CH$_2$C(CH$_3$)C(CH$_3$)-CH$_2$B(C$_6$F$_5$)$_3$) (18). Compound **17** (148 mg, 0.313 mmol) and $B(C_6F_5)_3$ (176 mg, 0.344 mmol) were placed into a reaction vial. Toluene (6 mL) was added to the solid mixture and the solution stirred at 25 °C overnight. The solution was decanted and the yellow solid was dried under vacuum. Yield: 208 mg (71%). ^{1}H NMR (tol-d_8): δ 2.21 (m, 2H, CH_2, J_{H-H} = 12 Hz), 1.79 (s, 15H, Cp*-CH_3), 1.60 (s, 3H, diene-CH_3), 1.52 (3H, diene-CH_3), 0.59 (d, 2H, CH_2, J_{H-H} = 15 Hz), 0.95 (d, 27H, *t*-Bu-CH_3, J_{P-H} = 15 Hz). ^{31}P{^{1}H} NMR (tol-d_8): δ 44.2. ^{11}B NMR (tol-d_8): 31.7. ^{19}F NMR (tol-d_8, 193 K): *m*-F, δ −127.8, −130.2, −131.1, −131.1, −133.1, −134.6, *p*-F, δ −158.7, −159.1, −160.3; *o*-F, δ −161.9, −162.9, −162.9, −163.7, −164.9, −166.2. The extreme sensitivity of this compound precluded elemental analysis; NMR data have been deposited as Supporting Information.

Generation of Cp*Zr(NP-*t*-Bu$_3$)(THF)$_n$(CH$_2$C(CH$_3$)C-(CH$_3$)CH$_2$B(C$_6$F$_5$)$_3$) (19). Compound **18** was dissolved in THF and characterized by NMR methods. ^{1}H NMR (THF-d_8): 2.36 (d, 1H, CH_2, J_{H-H} = 13 Hz), 2.22 (d, 1H, CH_2, J_{H-H} = 13 Hz), 2.06 (s, 15H, Cp*-CH_3), 1.56 (d, 3H, diene-CH_3, J_{H-H} = 14 Hz), 1.46 (d, 27H, CH_3, J_{P-H} = 13 Hz), 1.35 (s, 3H, CH_3), 0.88 (br. m, 1H, CH_2, J_{H-H} = 13 Hz), 0.82 (d, 1H, CH_2, J_{H-H} = 11 Hz). ^{31}P{^{1}H} NMR (THF-d_8): 46.5. ^{13}C{^{1}H} NMR (THF-d_8): 128.5 (d, J_{P-C} = 57 Hz), 122.0, 78.8, 40.4 (d, J_{P-C} = 45 Hz), 34.4, 29.3, 28.1, 21.8, 19.1, 11.1. ^{11}B{^{1}H} NMR (THF-d_8): 28.5. ^{19}F-{^{1}H} NMR (THF-d_8): −130.1 (s, *o*-C_6F_5), −165.7 (t, *m*-C_6F_5), −168.4 (t, *p*-C_6F_5). The extreme sensitivity of this compound precluded elemental analysis; NMR data have been deposited as Supporting Information.

Synthesis of CpZr(NP-*t*-Bu$_3$)(C$_6$F$_5$)$_2$ (20). This compound was obtained in two ways. (i) A solution of C_6F_5MgBr (2.8 mmol) in Et_2O was added dropwise at 25 °C to a slurry of **1** (0.25 g, 0.56 mmol) in the same solvent (80 mL). The heterogeneous mixture was stirred for 15 h, after which time the solvent was removed in vacuo. The product was extracted with PhH (3 × 20 mL) and filtered through Celite. Following removal of solvent, the brown residue was washed with hexanes (3 × 5 mL), filtered, and dried in vacuo to afford a pale gray solid (0.32 g, 81%).

(ii) Solid **4** (36 mg, 0.089 mmol) and $B(C_6F_5)_3$ (46 mg, 0.089 mmol) were combined in a dry vial. Subsequent addition of benzene (2 mL) resulted in a heterogeneous solution, which grew clear within 1 min. After the mixture was stirred for 30 min, the solvent was removed in vacuo and the residue was washed with hexanes (56 mg, 89%). ^{1}H NMR (C_6D_6): δ 6.41 (s, 5H, C_5H_5), 0.94 (d, 27H, J_{P-H} = 6 Hz, $(CH_3)_3$−C−). ^{13}C{^{1}H} NMR (C_6D_6): δ 148.0 (dd, J_{C-F} = 220 Hz, J_{C-F} = 30 Hz, C_6F_5 (*o*-C)), 140.6 (dd, J_{C-F} = 240 Hz, J_{C-F} = 15 Hz, C_6F_5 (*p*-C)), 140.1 (s, C_6F_5 (ipso-C)), 136.8 (ddd, J_{C-F} = 260 Hz, J_{C-F} = 30 Hz, J_{C-F} = 15 Hz, C_6F_5 (*m*-C)), 112.5 (s, C_5H_5), 39.9 (d, J_{P-C} = 45 Hz, $(CH_3)_3$−C), 28.9 (s, $(CH_3)_3$−C). ^{19}F{^{1}H} NMR (C_6D_6): δ −118.7 (m, 4F, *o*-F), −154.5 (t, 2F, J_{F-F} = 20 Hz, *p*-F), −161.5 (m, 4F, *m*-F). ^{31}P{^{1}H} NMR (C_6D_6): δ 42.7 (s). Anal. Calcd for $C_{29}H_{32}F_{10}NPZr$: C, 49.28; H, 4.56; N, 1.98. Found: C, 49.10; H, 4.37; N, 1.74.

Reaction of 2 with AlMe$_3$. (i) To a yellow benzene solution (0.5 mL) of **2** (100 mg; 0.21 mmol) was added a 2.5 M hexanes solution (0.42 mL, 1.06 mmol) of $AlMe_3$. The color of the solution changed from yellow to red after it was left in an NMR tube overnight. NMR data revealed the formation of a complex mixture of products. A few crystals of **21** suitable for X-ray crystallography were obtained. This species was identified by $(Cp^*Zr)_4(\mu\text{-}Cl)_5(Cl)(\mu\text{-}CH)_2\cdot 0.5C_6H_6$ (**21**). Yield: <5%. ^{1}H NMR (C_6D_6): δ 14.29 (s, 2H, CH), 2.06 (s, 15H, CH_3), 1.97 (s, 30H, CH_3), 1.95 (s, 15H, CH_3). ^{13}C{^{1}H} NMR (C_6D_6): partial, 123.5, 120.1, 13.8, 13.3, 12.8.

(ii) To a turbid yellow solution of 136 mg (0.288 mmol) of **2** in 0.5 mL of C_6D_6 was added dropwise 0.14 mL (1.44 mmol) of $AlMe_3$. The color of the solution changed from yellow to red after it was left in an NMR tube overnight. NMR data revealed the formation of a complex mixture of products. After 3 days, red crystals suitable of **22** suitable for X-ray crystallography were obtained. This species was identified as $(Cp^*Zr)_5(\mu\text{-}Cl)_6(\mu\text{-}CH)_3\cdot C_6H_6$ (**22**). Yield: <5%. ^{1}H NMR (C_6D_6): δ 14.4 (s, 2H, CH), 9.34 (s, 1H, CH), 2.06 (s, 15H, CH_3), 1.97 (s, 15H, CH_3), 1.93 (s, 30H, CH_3), 1.83 (s, 15H, CH_3). ^{13}C{^{1}H} NMR (C_6D_6): δ 372.9 (s, 2 CH), 168.3 (s, CH), 120.8, 119.6, 118.1, 14.45, 13.6, 13.4, 13.3.

Ethylene Polymerization. (i) A solution of 6−10 μmol of catalyst precursor in 2.0 mL of dry toluene was added to a flask containing 2.0 mL of dry toluene. A 500 equiv amount of a 10 wt % toluene solution of MAO was added to the flask. Alternatively, the catalyst precursors were combined with $[Ph_3C][B(C_6F_5)_4]$ under an ethylene atmosphere at 25 °C. The flask was attached to a Schlenk line with a cold trap, a stopwatch was started, and the flask was evacuated three times for 5 s and refilled with predried 99.9% ethylene gas. The solution was rapidly stirred under 1 atm of ethylene at room temperature. The polymerization was stopped by the injection of a 1.0 N HCl/methanol solution. The total reaction time was noted, and the polymer was isolated.

(ii) A typical experiment is as follows: a 1 L autoclave was dried under vacuum (10^{-2} mmHg) for several hours. Toluene (500 mL) was transferred into the vessel under a positive pressure of N_2 and was heated to 30 °C. The temperature was controlled (to ca. ±2 °C) with an external heating/cooling bath and was monitored by a thermocouple that extended into the polymerization vessel. A solution of MAO (500 equiv) in toluene was injected, and the mixture was stirred for 3 min at a rate of 150 rpm. The precatalyst in a solution of toluene was then injected while the reaction mixture was stirred for 3 min at the same rate. The rate of stirring was increased to 1000 rpm, and the vessel was vented of N_2 and pressurized with ethylene (33 psi). Any recorded exotherm was within the allowed temperature differential of the heating/cooling system. The solution was stirred for 1 h, after which time the reaction was quenched with 1 M HCl in MeOH. The precipitated polymer was subsequently washed with MeOH and dried at 100 °C for at least 24 h prior to weighing.

X-ray Data Collection and Reduction. X-ray-quality crystals were obtained directly from the preparation as described above. The crystals were manipulated and mounted in capillaries in a glovebox, thus maintaining a dry, O_2-free environment for each crystal. Diffraction experiments were performed on a Siemens SMART System CCD diffractometer. The data were collected for a hemisphere of data in 1329 frames with 10 s exposure times. Crystal data are summarized in Table 1. The observed extinctions were consistent with the space groups in each case. A measure of decay was obtained by re-collecting the first 50 frames of each data set. The intensities of reflections within these frames showed no

Table 1. Crystallographic Parameters

	1	**2**	**6**	**9**	**13**	**15**	**16**	**17**	**22**	**23**
formula	$C_{17}H_{32}Cl_2NPZr$	$C_{19}H_{36}Cl_2NPZr$	$C_{24}H_{35}NPZr$	$C_{34}H_{52}NPZr$	$C_{28}H_{52}NPZr$	$C_{24}H_{41}ClNPZr$	$C_{25}H_{46}NPZr$	$C_{28}H_{52}NPZr$	$C_{45}H_{64}Cl_6Zr_4$	$C_{59}H_{84}Cl_6Zr_5$
fw	443.53	471.58	459.72	596.96	524.90	501.22	482.82	524.90	1182.54	1462.06
a (Å)	10.252(2)	8.275(2)	8.5914(11)	16.8506(2)	8.75600(10)	8.2990(1)	9.3541(2)	10.4976(3)	19.8881(2)	13.5603(17)
b (Å)	14.886(3)	15.282(5)	14.587(3)	11.44601(1)	11.6427(2)	15.2858(3)	17.8965(4)	15.9192(4)	14.5373(3)	13.8668(17)
c (Å)	28.717(6)	19.690(5)	21.600(2)	33.7035(5)	15.8052(1)	20.3234(1)	16.5357(3)	17.7561(4)	18.0578(2)	32.055(4)
α (deg)	90	90	90	90	101.015(1)	90	90	90	90	90
β (deg)	90	90	91.110(12)	102.803(1)	90.495(1)	98.360(1)	102.319(1)	96.213(1)	106.69(1)	96.248(2)
γ (deg)	90	90	90	90	110.786(1)	90	90	90	90	90
cryst syst	orthorhombic	orthorhombic	monoclinic	monoclinic	triclinic	monoclinic	monoclinic	monoclinic	monoclinic	monoclinic
space group	*Pbca*	$P2_12_12_1$	$P2_1/c$	$P2_1/n$	$P\bar{1}$	$P2_1/n$	$P2_1/c$	$P2_1/n$	$P2_1/c$	$P2_1/c$
V (Å^3)	4382.6(16)	2490.0(12)	1706.5(7)	6339.01(12)	1473.47(3)	2550.78(6)	2704.4(1)	2949.85(13)	5000.94(13)	5991.8(13)
D_{calcd} (g cm^{-3})	1.344	1.258	1.128	1.251	1.183	1.305	1.186	1.182	1.571	1.621
Z	8	4	4	8	2	4	4	4	4	4
abs coeff, μ, cm^{-1}	0.816	0.722	0.473	0.419	0.442	0.608	0.476	0.441	1.160	1.145
2θ range (deg)	1.69−25.00	1.69−25.00	1.69−25.00	1.26−25.00	1.91−25.00	1.67−24.99	2.23−25.00	1.72−25.00	1.72−25.00	1.72−25.00
no. of rflns collected	17 365	12 905	10 000	31 839	7696	11 967	13 553	13 957	17 097	13 349
R_{int}	0.0244	0.0488	0.0171	0.043	0.0119	0.2171	0.0272	0.0662	0.1157	0.0598
no. of data with $F_o^2 > 3\sigma(F_o^2)$	3152	4350	4641	11 015	5032	4466	4690	5056	5354	8060
no. of params	199	217	244	667	280	253	253	280	391	643
R (%)[a]	0.0657	0.0658	0.0393	0.0514	0.0433	0.0636	0.0386	0.0612	0.1212	0.0511
R_w (%)[a]	0.1638	0.1590	0.1359	0.1400	0.1191	0.1079	0.1171	0.1199	0.2071	0.1039
goodness of fit	1.167	1.066	1.198	0.750	1.046	0.467	0.954	1.026	1.388	0.867

[a] $R = \sum||F_o| - |F_c||/\sum|F_o|$, $R_w = [\sum(|F_o| - |F_c|)^2]/\sum|F_o|^2]^{0.5}$.

Figure 1. ORTEP drawing of **1**. Thermal ellipsoids at the 30% level are shown; hydrogen atoms have been omitted for clarity. Selected bond distances (Å) and angles (deg): Zr(1)−N(1) = 1.902(5), Zr(1)−Cl(1) = 2.410(2), Zr(1)−Cl(2) = 2.418(2), P(1)−N(1) = 1.588(5); N(1)−Zr(1)−Cl(1) = 105.42(18), N(1)−Zr(1)−Cl(2) = 103.27(18), Cl(1)−Zr(1)−Cl(2) = 105.02(13), P(1)−N(1)−Zr(1) = 174.8(4).

statistically significant change over the duration of the data collections. An empirical absorption correction based on redundant data was applied to each data set. Subsequent solution and refinement was performed using the SHELXTL solution package.

Structure Solution and Refinement. Non-hydrogen atomic scattering factors were taken from the literature tabulations.[14] The heavy-atom positions were determined using direct methods. The remaining non-hydrogen atoms were located from successive difference Fourier map calculations. The refinements were carried out by using full-matrix least-squares techniques on *F*, minimizing the function $\omega(|F_o| - |F_c|)^2$, where the weight ω is defined as $4F_o^2/2\sigma(F_o^2)$ and F_o and F_c are the observed and calculated structure factor amplitudes. For noncentrosymmetric space groups, the correct enantiomorphic was confirmed by data inversion and refinement. In the final cycles of each refinement, all non-hydrogen atoms were assigned anisotropic temperature factors. Carbon-bound hydrogen atom positions were calculated and allowed to ride on the carbon to which they are bonded, assuming a C−H bond length of 0.95 Å. Hydrogen atom temperature factors were fixed at 1.10 times the isotropic temperature factor of the carbon atom to which they are bonded. The hydrogen atom contributions were calculated but not refined. The final values of refinement parameters are given in Table 1. Positional parameters, hydrogen atom parameters, thermal parameters, and bond distances and angles have been deposited as Supporting Information.

Results and Discussion

Zirconium phosphinimide complexes are readily prepared under ambient conditions via the reaction of $[CpZrCl_3]_n$ or Cp^*ZrCl_3 with the appropriate trialkylphosphinimide lithium salt (R_3PNLi). In this manner, the compounds $CpZr(NP\text{-}t\text{-}Bu_3)Cl_2$ (**1**) and $Cp^*Zr(NPR_3)Cl_2$ (R = *i*-Pr (**2**), *t*-Bu (**3**)) were obtained in good yields. While spectroscopic data were consistent with these formulations, X-ray crystallographic data confirmed the pseudo-tetrahedral geometry of the Zr coordination spheres in **1** and **2** (Figures 1 and 2). In both cases the P−N−Zr angles were approaching linearity, being

(14) Cromer, D. T.; Mann, J. B. *Acta Crystallogr., Sect. A* **1968**, *A24*, 321−324.

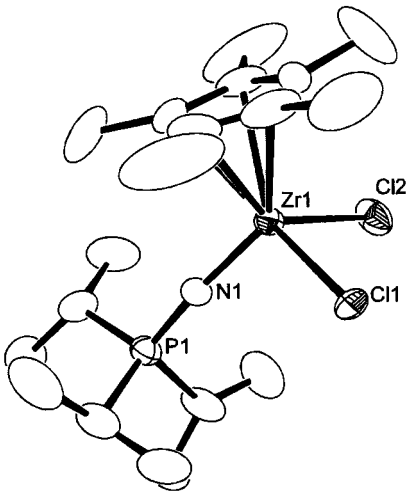

Figure 2. ORTEP drawing of **2**. Thermal ellipsoids at the 30% level are shown; hydrogen atoms have been omitted for clarity. Selected bond distances (Å) and angles (deg): Zr(1)−N(1) = 1.926(7), Zr(1)−Cl(1) = 2.581(2), Zr(1)−Cl(2) = 2.559(3), P(1)−N(1) = 1.569(7); P(1)−N(1)−Zr(1) = 175.2(4), Cl(2)−Zr(1)−Cl(1) = 94.70(10), N(1)−Zr(1)−Cl(1) = 104.7(2), N(1)−Zr(1)−Cl(2) = 104.0(2).

174.8(4) and 175.2(4)° in **1** and **2**, respectively. These are much larger than those reported for the related dimeric ($[Zr_2Cl_4(NPMe_3)_4(\mu\text{-}HNPMe_3)]$) (159.3(2), 155.6(2)°)[15] and trimeric ($[Zr_3Cl_6(NPMe_3)_5]^+$) (132.9(7), 126.1(6)°)[16] species. The P−N bond distances of 1.588(5) and 1.569(7) Å, respectively, are typical of those found in other group IV phosphinimide complexes.[17] The Zr−N bond distances of 1.902(5) and 1.926(7) Å in **1** and **2**, respectively, are significantly shorter than the Zr−N bond distances found in the dimeric and trimeric species (1.95(2)−2.27(9) Å).[15−17] This suggests some degree of Zr−N multiple bond character.

A series of derivatives are readily obtained via alkylation or arylation of the above dihalide precursors. For example, the dimethyl derivatives $CpZr(NP\text{-}t\text{-}Bu_3)Me_2$ (**4**) and $Cp^*Zr(NPR_3)Me_2$ (R = *i*-Pr (**5**), *t*-Bu (**6**)) were readily isolated in high yields via reaction of the dihalide precursor with a methyl Grignard reagent. Spectroscopic data were consistent with dimethylation, and this was confirmed crystallographically in the case of **6** (Figure 3). The P−N−Zr angle (168.5(2)°), P−N bond distance (1.574(2) Å), and Zr−N bond distance (1.955(2) Å) in **6** is a reflection of a slightly lesser degree of Zr−N multiple-bond character, presumably arising from the presence of the electron-donating methyl groups.

In a similar synthetic route, the aryl derivatives $CpZr(NP\text{-}t\text{-}Bu_3)Ph_2$ (**7**) and $Cp^*Zr(NPR_3)Ph_2$ (R = *i*-Pr (**8**), *t*-Bu (**9**)) were obtained in 79−84% yield via reaction of the dichloride precursors with a phenyl Grignard reagent. Single crystals of **9** were crystallographically characterized (Figure 4). The metric parameters were similar to those observed for **6**. Similar alkylation of **1** with benzyl Grignard or (trimethylsilyl)methyl Grignard reagents afford the species $CpZr(NP\text{-}t\text{-}Bu_3)Bn_2$ (**10**) and $CpZr(NP\text{-}t\text{-}Bu_3)(CH_2SiMe_3)_2$ (**11**), respectively.

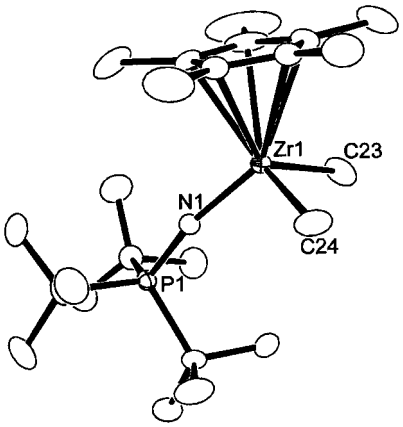

Figure 3. ORTEP drawing of **6**. Thermal ellipsoids at the 30% level are shown; hydrogen atoms have been omitted for clarity. Selected bond distances (Å) and angles (deg): P(1)−N(1) = 1.574(2), Zr(1)−N(1) = 1.955(2), Zr(1)−C(23) = 2.258(4), Zr(1)−C(24) = 2.265(4); N(1)−Zr(1)−C(23) = 104.4(2), N(1)−Zr(1)−C(24) = 103.8(2), P(1)−N(1)−Zr(1) = 168.5(2).

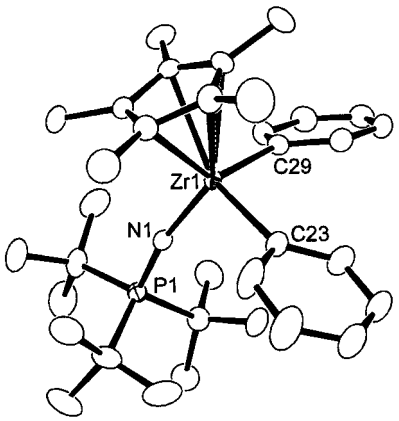

Figure 4. ORTEP drawing of one of the two molecules in the asymmetric unit of **9**. Thermal ellipsoids at the 30% level are shown; hydrogen atoms have been omitted for clarity. Selected bond distances (Å) and angles (deg): Zr(1)−N(1) = 1.922(4), Zr(1)−C(29) = 2.251(5), Zr(1)−C(23) = 2.268(4), P(1)−N(1) = 1.551(4); N(1)−Zr(1)−C(29) = 104.16(17), N(1)−Zr(1)−C(23) = 102.38(17), C(29)−Zr(1)−C(23) = 105.11(18), P(1)−N(1)−Zr(1) = 168.2(2).

Reactions of allyl Grignard reagent with **2** and **3** gave complexes of the formulation $Cp^*Zr(NPR_3)(allyl)_2$ (R = *i*-Pr (**12**), *t*-Bu (**13**)) in 71 and 73% yields, respectively. The ^1H NMR spectra at 25 °C for complexes **12** and **13** clearly showed a quintet and doublet attributable to the methine and methylene portions of symmetrically bound allyl fragments, inferring bis-η^3 binding. When the temperature is lowered to −80 °C, these resonances simply broadened, hinting that allyl group interconversion between η^1- and η^3-bound forms may be occurring rapidly. The X-ray structure of complex **13** revealed that in the solid state, both η^1- and η^3-bound allyl moieties are present (Figure 5). Thus, the coordination sphere of the chiral Zr center is comprised of the η^5-pentamethylcyclopentadienyl ligand, the phosphinimide ligand, and the two differently bonded allyl groups in a pseudo-tetrahedral geometry. One allyl group (C(26)−C(27)−C(28)) is bound solely through C(26) (Zr−C = 2.378(4) Å), while the second is η^3-bound, with Zr−C distances of 2.488(6), 2.543(6), and 2.378(4) Å.

(15) Stahl, M. M.; Faza, N.; Massa, W.; Dehnicke, K. *Z. Anorg. Allg. Chem.* **1997**, *623*, 1855−1856.
(16) Grün, M.; Weller, F.; Dehnicke, K. *Z. Anorg. Allg. Chem.* **1997**, *623*, 224.
(17) Dehnicke, K.; Krieger, M.; Massa, W. *Coord. Chem. Rev.* **1999**, *182*, 19−65.

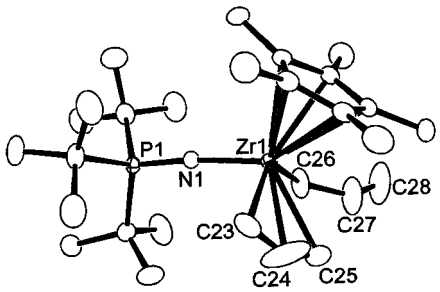

Figure 5. ORTEP drawing of **13**. Thermal ellipsoids at the 30% level are shown; hydrogen atoms have been omitted for clarity. Selected bond distances (Å) and angles (deg): Zr(1)−N(1) = 1.976(2), Zr(1)−C(23) = 2.490(5), Zr(1)−C(24) = 2.488(6), Zr(1)−C(25) = 2.543(6), Zr(1)−C(26) = 2.378(4), P(1)−N(1) = 1.588(2), C(23)−C(24) = 1.358(13), C(24)−C(25) = 1.165(13), C(26)−C(27) = 1.440(7), C(27)−C(28) = 1.163(9); P(1)−N(1)−Zr(1) = 173.56(16), N(1)−Zr(1)−C(23) = 94.20(13), N(1)−Zr(1)−C(24) = 107.7(4), N(1)−Zr(1)−C(25) = 118.8(2), N(1)−Zr(1)−C(26) = 92.27(12).

The "mixed-ring" complexes Cp*Zr(NPR$_3$)(Cp)Cl (R = *i*-Pr (**14**), *t*-Bu (**15**)) were also prepared cleanly from the reaction of sodium cyclopentadienide and **2** or **3**, respectively. The proposed η^5 coordination of both the pentamethylcyclopentadienyl and the cyclopentadienyl ligands was supported by spectroscopic data and confirmed crystallographically in the case of compound **15** (Figure 6).

Reaction of the compounds Cp*Zr(NPR$_3$)Cl$_2$ (R = *i*-Pr (**2**), *t*-Bu (**3**)) with Mg powder in THF resulted in a color change to dark blue. Subsequent addition of 1 equiv of 2,3-dimethyl-1,3-butadiene afforded, after 12 h of stirring and typical workup, a new orange species formulated as Cp*Zr(NPR$_3$)(CH$_2$C(CH$_3$)C(CH$_3$)CH$_2$) (R = *i*-Pr (**16**), *t*-Bu (**17**)) in approximately 75% isolated yield. Each of these species exhibited a single resonance in the ^{31}P{^{1}H} NMR spectra, as was expected. Similarly, the ^{1}H and ^{13}C{^{1}H} NMR data were also consistent with the above formulations. Nonetheless, a number of possible isomers of these products are conceivable.[18,19] These include cis and trans conformations of the butadiene, in addition to the prone (**A**) and supine (**B**)

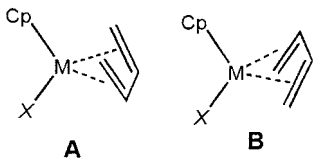

isomers, which differ only with respect to the orientation of the butadiene ligand in relation to the pentamethylcyclopentadienyl and phosphinimide ligands. At ambient temperature, two doublets of equal intensity were observed in the ^{1}H NMR spectra of **16** and **17** and were attributed to the terminal CH$_2$ of the diene. The lower and higher field resonances of these were assigned to the syn and anti protons, respectively. This is consistent with shielding of the anti protons by the proximal pentamethylcyclopentadienyl ligand.

(18) Yasuda, H.; Tatsumi, K.; Nakmura, A. *Acc. Chem. Res.* **1985**, *18*, 120−126.
(19) Yasuda, H.; Nakamura, A. *Angew. Chem., Int. Ed. Engl.* **1987**, *26*, 723−742.

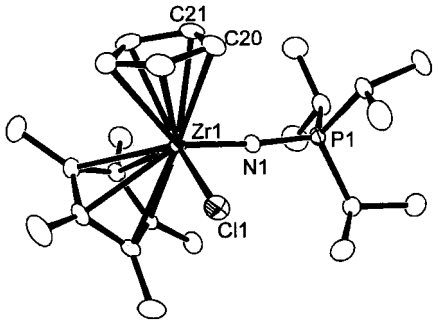

Figure 6. ORTEP drawing of **15**. Thermal ellipsoids at the 30% level are shown; hydrogen atoms have been omitted for clarity. Selected bond distances (Å): Zr(1)−N(1) = 1.976(2), Zr(1)−Cl(1) = 2.5070(8).

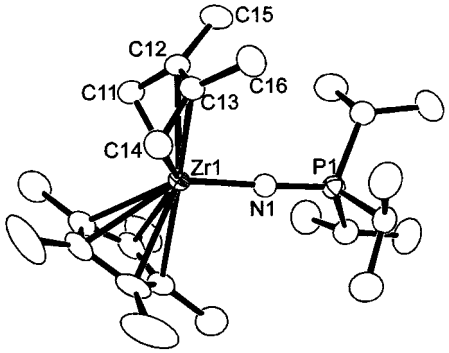

Figure 7. ORTEP drawing of **16**. Thermal ellipsoids at the 30% level are shown; hydrogen atoms have been omitted for clarity. Selected bond distances (Å) and angles (deg): Zr(1)−N(1) = 1.982(3), P(1)−N(1) = 1.564(3), Zr(1)−C(11) = 2.282(3), Zr(1)−C(12) = 2.533(3), Zr(1)−C(13) = 2.538(3), Zr(1)−C(14) = 2.288(3), C(11)−C(12) = 1.454(5), C(12)−C(13) = 1.383(5), C(13)−C(14) = 1.455(5); C(11)−Zr(1)−C(14) = 80.05(14), P(1)−N(1)−Zr(1) = 173.52(17).

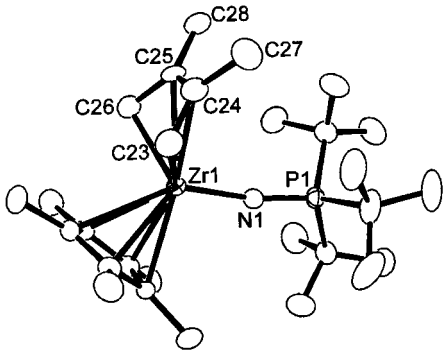

Figure 8. ORTEP drawing of **17**. Thermal ellipsoids at the 30% level are shown; hydrogen atoms have been omitted for clarity. Selected bond distances (Å) and angles (deg): Zr(1)−N(1) = 1.996(4), P(1)−N(1) = 1.576(4), Zr(1)−C(23) = 2.258(6), Zr(1)−C(24) = 2.638(6), Zr(1)−C(25) = 2.642(5), Zr(1)−C(26) = 2.269(5), C(23)−C(24) = 1.462(9), C(24)−C(25) = 1.390(9), C(25)−C(26) = 1.476(8); C(23)−Zr(1)−C(26) = 80.5(2), P(1)−N(1)−Zr(1) = 169.3(3).

While the above NMR data were consistent with the presence of only one isomer in solution, the precise nature of these Zr compounds was unambiguously confirmed via X-ray crystallographic studies (Figures 7 and 8). In both cases, the structural data reveal that the coordination of the Zr center is comprised of pentamethylcyclopentadienyl, phosphinimide, and *cis*-butadiene ligands, such that the butadiene substituents are

oriented away from the pentamethylcyclopentadienyl ligand: that is, in a supine conformation. The Zr−C distances for the α- and β-butadiene carbons average 2.285(3) and 2.534(3) Å in **16**, while the corresponding averages are 2.640(5) and 2.263(6) Å in **17**, respectively. The butadiene ligand clearly makes a closer approach to the Zr in **16** than in **17**, consistent with changes in the steric demands and donor abilities of the phosphinimide ligands. However, the corresponding Zr−N distances appear to be dominated by steric effects, as the Zr−N distance in **16** (1.982(3) Å) is slightly longer than that in **17** (1.996(4) Å). It is also noteworthy that the C−C distances of the central bond of the butadiene ligands are 1.383(5) and 1.390(9) Å in **16** and **17**, respectively. In addition, the dihedral angle between the planes containing the four carbons of the butadiene ligand and that consisting of Zr and the two α-carbons are 116.5 and 108.7° for **16** and **17**, respectively. These data infer that the Zr−butadiene interaction is best described as a σ^2,π-bonded η^4 interaction. These structural parameters of the butadiene moieties are typical of those seen for a number of other early metal butadiene complexes.[18,19]

A number of previously characterized metallocene−butadiene complexes[18−25] exhibit fluxional behavior. For example, Erker et al.[23] have observed and determined the energetics of equilibrium processes involving both cis−trans isomerization of the butadiene as well as ring flipping (eq 1). In the case of compounds **16** and **17**,

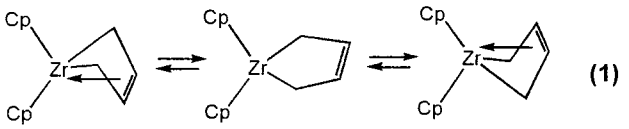

(1)

variable-temperature ^{1}H NMR studies reveal only a slight broadening of the resonances attributable to the butadiene moieties. The dissymmetry of these phosphinimide complexes presumably generates a significant thermodynamic preference for the supine conformation, thus providing a significant barrier to ring inversion. While the butadiene fragments are temperature-invariant, the signals arising from the *tert*-butyl groups in compounds **17** did show a temperature dependence. At room temperature, the ^{1}H resonance is the predicted doublet arising from coupling to phosphorus. Upon cooling, the resonance broadens and splits into two peaks in a ratio of 2:1. The coalescence occurs at approximately −55 °C in each case. These observations are consistent with restricted rotation about the Zr−N bond, due to a cogwheel effect of the *tert*-butylphosphinimide and pentamethylcyclopentadienyl groups. It is noteworthy that we have recently described similar observations for the species Cp*Ta(NP-*t*-Bu$_3$)X$_3$ (X = Cl, Me).[9] The complexity of this fluxional behavior precluded analysis and the determination of associated kinetic and thermodynamic data.

Zwitterionic Complexes. The reactions of **17** with B(C$_6$F$_5$)$_3$ in toluene results in the formation of the yellow betaine complex Cp*Zr(NP-*t*-Bu$_3$)(CH$_2$C(CH$_3$)C(CH$_3$)-CH$_2$B(C$_6$F$_5$)$_3$) (**18**) in 71% yield. The ^{1}H NMR resonances at δ 2.21 and 0.59 are attributable to methylene groups bonded to the formal cationic Zr and anionic B centers, respectively. The ^{19}F NMR spectrum exhibits the inequivalence of the 15 fluorine environments. Given that *cis*-diene complexes are known to react with B(C$_6$F$_5$)$_3$ to give dienylborate species with a linear Zr−C−B dipole, we attribute the observed inequivalence to inhibited rotation about the B−C bonds. This contrasts with the *trans*-butadiene complex Cp$_2$Zr(CH$_2$CHCH-CH$_2$B(C$_6$F$_5$)$_3$), where Karl et al.[26] observed 15 inequivalent ^{19}F NMR resonances with an interaction of an ortho fluorine with the cationic Zr, resulting in the observation of one ^{19}F resonance that is dramatically shifted downfield. In this case, a Zr−F interaction was confirmed crystallographically (eq 2); however, the precise orienta-

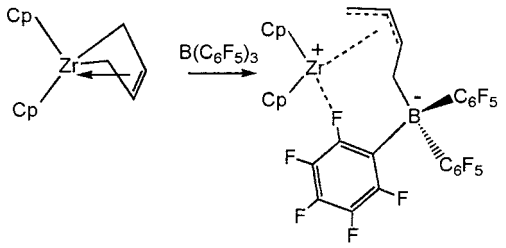

(2)

tion of the aryl groups in **18** remains unknown in the absence of crystallographic data. However, a structurally related half-sandwich species (C$_5$H$_3$(SiMe$_3$)$_2$)Hf-(C$_3$H$_5$)(CH$_2$CMeCMeCH$_2$B(C$_6$F$_5$)$_3$) has been reported by Bochmann et al.[27] It is worth mentioning that dissolution of **18** in THF affords the species Cp*Zr(NP-*t*-Bu$_3$)-(THF)$_n$(CH$_2$C(CH$_3$)C(CH$_3$)CH$_2$B(C$_6$F$_5$)$_3$) (**19**). In this species, THF coordination to Zr presumably results in an η^1 binding mode of the butadienyl−borate, allowing unrestricted rotation of the borate fragment, as evidenced by the presence of only three ^{19}F{^{1}H} NMR resonances.

Ethylene Polymerization. A number of the above compounds were screened for their potential as catalyst precursors in ethylene polymerizations. These tests were performed either using the known route of combining early metal dichloride complexes with excess methylalumoxane (MAO) or employing corresponding dialkyl species and either MAO or trityl tetrakis-(pentafluorophenyl)borate as the activator. Reaction conditions of 1 atm of ethylene at 25 °C or 33 psig of ethylene and 30 °C were employed. The nature of the tests reported herein is tabulated in Table 2. In general, the compounds described herein are poor ethylene polymerization catalysts in comparison to the related Titanium species,[2,3] although the activities were increased somewhat under elevated temperatures and pressures. The cause of this marked difference may be related to the significantly larger ionic radius of Zr,

(20) Kruger, C.; Muller, G. *Organometallics* **1985**, *4*, 215−223.
(21) Dorf, U.; Engel, K.; Erker, G. *Organometallics* **1983**, *2*, 462−463.
(22) Erker, G.; Dorf, U.; Benn, R.; Reinhardt, R.-D. *J. Am. Chem. Soc.* **1984**, *106*, 7649−7650.
(23) Erker, G.; Wicher, J.; Engel, K.; Rosenfeldt, F.; Dietrich, W. *J. Am. Chem. Soc.* **1980**, *102*, 6344−6346.
(24) Wreford, S. S.; Whitney, J. F. *Inorg. Chem.* **1981**, *20*, 3918−3924.
(25) Fujita, K.; Ohnuma, Y.; Yasuda, H.; Tani, H. *J. Organomet. Chem.* **1976**, *113*, 201−213.
(26) Karl, J.; Erker, G.; Fohlich, R. *J. Am. Chem. Soc.* **1997**, *119*, 11165−11173.
(27) Pindado, G. J.; Thornton-Pett, M.; Bochmann, M. *J. Chem. Soc., Dalton Trans.* **1997**, 3115−3127.

Table 2. Ethylene Polymerization Data

catalyst precursor	cocatalyst[a]	time (min)	productivity (g mmol^{-1} h^{-1})	M_w	M_w/M_n
1[b]	MAO	30.0	11	94,300	2.6
1[c]	MAO	60.0	100	234,000	67.9
2[b]	MAO	30.0	*d*		
3[b]	MAO	30.0	*d*		
4[b]	MAO	60.0	43		
2[c]	MAO	60.0	1	506,400	41.5
3[c]	MAO	60.0	48	9220	3.3
4[c]	MAO	60.0	87	49,900	33.5
5[b]	TB	3.00	*d*		
6[b]	TB	3.00	*d*		
16[b]	TB	3.00	181	132,300	4.4
17[b]	TB	3.00	*d*		
Cp_2ZrCl_2b	MAO	2.00	895	116,353	2.8

[a] Abbreviations: MAO, methylaluminoxane (500 equiv); TB, trityl tetrakis(pentafluorophenyl)borate (1 equiv). [b] Polymerizations were run at 1 atm pressure of ethylene and 25 °C. [c] Polymerizations were run at 33 psi pressure of ethylene, 30 °C. Molecular weight data were recorded against polyethylene standards. [d] Too little polymer to determine accurately.

which facilitates deactivation pathways over chain propagation.

Deactivation Pathways. Efforts to understand the deactivation pathway for these zirconium catalysts were undertaken. Zwitterionic complexes analogous to those reported for both titanium phosphinimide species[2,3,5] and metallocene derivatives[28,29] are readily prepared using the now conventional approach of reaction of an alkyl-complex with the Lewis acid $B(C_6F_5)_3$. However, reaction of **4** with this borane did not yield the expected zwitterion; rather, the quantitative product of aryl group transfer $CpZr(NP\text{-}t\text{-}Bu_3)(C_6F_5)_2$ (**20**) was formed as evidenced by multinuclear NMR spectral data. This interpretation was confirmed by the independent synthesis of **20** from **1** and the Grignard reagent $BrMgC_6F_5$. This observation stands in contrast to the analogous Ti reaction, which readily affords the zwitterionic species $CpTi(NP\text{-}t\text{-}Bu_3)(CH_3)(\mu\text{-}CH_3B(C_6F_5)_3)$,[3] suggesting that the increase in the metal atom size prompts the observed alkyl for aryl exchange. Similar C_6F_5 transfer reactions have been previously observed.[5,30,31] Moreover, this observation offers an explanation for the markedly low catalytic activity in comparison with the Ti analogues,[3] suggesting a chemical pathway for deactivation of the catalyst precursor.

In modeling the interaction of the dichloride complexes with MAO, the reaction of **2** with $AlMe_3$ was studied. Monitoring the ^{31}P NMR spectra for this reaction indicated the formation of complex mixture of products. While the nature of these phosphorus-containing products remains unknown, two Zr-containing products could be recrystallized in very low yields from reactions under slightly varied conditions. The species **21** and **22** were characterized by NMR and X-ray methods. Compound **21**, obtained from the reaction of **2** with $AlMe_3$ in benzene/hexane, exhibited ^1H NMR data consistent with three pentamethylcyclopentadienyl ligand environments in a 1:2:1 ratio. X-ray methods confirmed the formulation of **21** as the Zr_4 cluster $(Cp^*Zr)_4(\mu\text{-}Cl)_5(Cl)(\mu\text{-}CH)_2$ (Figure 9). This species is comprised of four Zr atoms bound to a central methine carbon (C52). Each of the Zr atoms are bonded to a pentamethylcyclopentadienyl ligand and two bridging chloride atoms. One of the Zr atoms has an additional terminal chloride, while the remaining three Zr atoms are bridged by an additional methine carbon (C51). The Zr−Cl distances range from 2.581(5) to 2.677(5) Å for the bridging chlorides, while the terminal Zr−Cl bond distance is 2.495(6) Å. There is also a close approach of Zr(1) to Cl(6) at 3.063(5) Å. The triply bridging methine carbon is approximately tetrahedral: C−Zr−C angles and Zr−C distances averaging 91.0(6)° and 2.263(18) Å, respectively. The geometry about the central carbon C(52) suggests a trigonal-bipyramidal Zr coordination sphere, as the Zr(1)−C(52)−Zr(4) angle is 164.1(9)° and

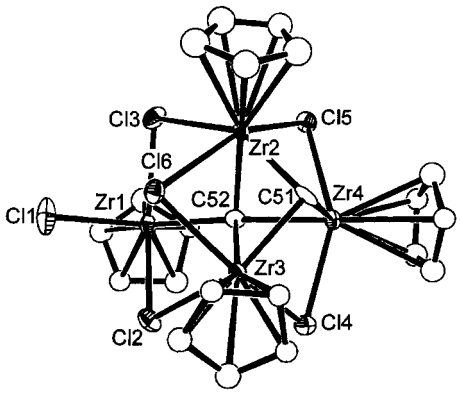

Figure 9. ORTEP drawing of **21**. Thermal ellipsoids at the 30% level are shown; the methyl carbons and hydrogen atoms have been omitted for clarity. Selected bond distances (Å) and angles (deg): Zr(1)−Cl(1) = 2.495(6), Zr(1)−Cl(2) = 2.583(6), Zr(1)−Cl(3) = 2.585(6), Zr(1)−Cl(6) = 3.063(5), Zr(2)−Cl(5) = 2.581(5), Zr(2)−Cl(6) = 2.637(5), Zr(2)−Cl(3) = 2.677(5), Zr(1)−C(52) = 2.197(19), Zr(2)−C(51) = 2.300(19), Zr(2)−C(52) = 2.33(2), Zr(3)−C(51) = 2.314(17), Zr(3)−C(52) = 2.327(16), Zr(3)−Cl(4) = 2.595(6), Zr(3)−Cl(6) = 2.613(6), Zr(3)−Cl(2) = 2.694(5), Zr(4)−C(51) = 2.177(16), Zr(4)−C(52) = 2.304(19), Zr(4)−Cl(4) = 2.591(6), Zr(4)−Cl(5) = 2.619(6); C(52)−Zr(1)−Cl(1) = 140.2(5), C(52)−Zr(1)−Cl(2) = 82.1(5), Cl(1)−Zr(1)−Cl(2) = 86.0(2), C(52)−Zr(1)−Cl(3) = 82.2(5), Cl(1)−Zr(1)−Cl(3) = 87.3(2), Cl(2)−Zr(1)−Cl(3) = 146.28(17), C(52)−Zr(1)−Cl(6) = 66.4(5), Cl(1)−Zr(1)−Cl(6) = 73.83(17), Cl(2)−Zr(1)−Cl(6) = 74.10(16), Cl(3)−Zr(1)−Cl(6) = 72.30(16), C(51)−Zr(2)−C(52) = 70.1(6), C(51)−Zr(2)−Cl(5) = 89.7(4), C(52)−Zr(2)−Cl(5) = 76.3(4), C(51)−Zr(2)−Cl(6) = 86.0(4), C(52)−Zr(2)−Cl(6) = 73.2(5), Cl(5)−Zr(2)−Cl(6) = 148.77(18), C(51)−Zr(2)−Cl(3) = 147.2(5), C(52)−Zr(2)−Cl(3) = 77.9(5), Cl(5)−Zr(2)−Cl(3) = 89.11(17), Cl(6)−Zr(2)−Cl(3) = 78.27(17), C(51)−Zr(3)−C(52) = 69.8(6), C(51)−Zr(3)−Cl(4) = 89.5(5), C(52)−Zr(3)−Cl(4) = 76.1(5), C(51)−Zr(3)−Cl(6) = 86.3(5), C(52)−Zr(3)−Cl(6) = 73.7(5), Cl(4)−Zr(3)−Cl(6) = 149.08(17), C(51)−Zr(3)−Cl(2) = 146.9(4), C(52)−Zr(3)−Cl(2) = 77.4(5), Cl(4)−Zr(3)−Cl(2) = 86.82(18), Cl(6)−Zr(3)−Cl(2) = 80.33(18), C(51)−Zr(4)−C(52) = 72.7(6), C(51)−Zr(4)−Cl(4) = 92.7(5), C(52)−Zr(4)−Cl(4) = 76.6(5), C(51)−Zr(4)−Cl(5) = 91.5(5), C(52)−Zr(4)−Cl(5) = 75.9(5), Cl(4)−Zr(4)−Cl(5) = 149.52(18), Zr(4)−C(51)−Zr(2) = 90.4(6), Zr(4)−C(51)−Zr(3) = 89.8(6), Zr(2)−C(51)−Zr(3) = 93.2(6), Zr(1)−C(52)−Zr(4) = 164.1(9), Zr(1)−C(52)−Zr(2) = 104.6(8), Zr(4)−C(52)−Zr(2) = 86.7(6), Zr(1)−C(52)−Zr(3) = 104.1(7), Zr(4)−C(52)−Zr(3) = 86.4(6), Zr(2)−C(52)−Zr(3) = 92.1(6).

(28) Yang, X.; Stern, C. L.; Marks, T. J. *J. Am. Chem. Soc.* **1991**, *113*, 3623.
(29) Bochmann, M.; Lancaster, S. J.; Hursthouse, M. B.; Malik, K. M. A. *Organometallics* **1994**, *13*, 2235.
(30) Scollard, J. D.; McConville, D. M.; Rettig, S. J. *Organometallics* **1997**, *16*, 1810.
(31) Woodman, T. J.; Bochmann, M.; Thornton-Pett, M. *Chem. Commun.* **2001**, 329−330.

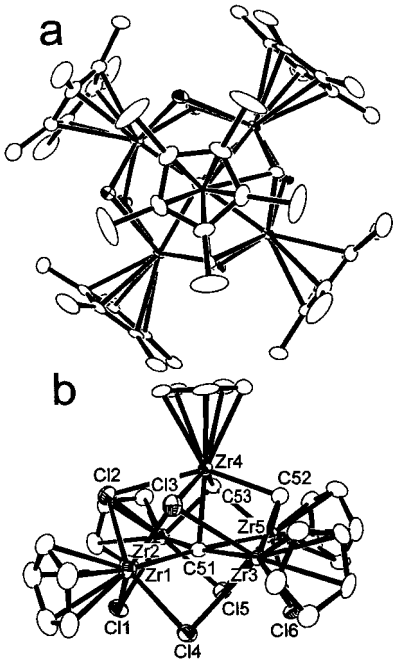

Figure 10. ORTEP drawings of **22**. Thermal ellipsoids at the 30% level are shown; hydrogen atoms have been omitted for clarity. The views (a) and (b) are approximately orthogonal; methyl carbons are omitted for clarity in (b). Selected bond distances (Å) and angles (deg): Zr(1)−C(51) = 2.349(8), Zr(1)−Cl(4) = 2.507(3), Zr(1)−Cl(1) = 2.536(3), Zr(1)−Cl(3) = 2.607(3), Zr(1)−Cl(2) = 2.647(3), Zr(2)−C(53) = 2.186(9), Zr(2)−C(51) = 2.412(9), Zr(2)−Cl(2) = 2.722(3), Zr(2)−Cl(1) = 2.746(3), Zr(3)−C(52) = 2.164(9), Zr(3)−C(51) = 2.410(10), Zr(3)−Cl(6) = 2.545(2), Zr(3)−Cl(4) = 2.774(2), Zr(3)−Cl(3) = 2.780(2), Zr(4)−C(52) = 2.235(9), Zr(4)−C(53) = 2.267(10), Zr(4)−C(51) = 2.324(10), Zr(4)−Cl(3) = 2.863(2), Zr(4)−Cl(2) = 2.917(3), Zr(5)−C(52) = 2.311(9), Zr(5)−C(53) = 2.331(9), Zr(5)−Cl(5) = 2.660(3), Zr(5)−Cl(6) = 2.690(2); C(51)−Zr(1)−Cl(4) = 79.3(2), C(51)−Zr(1)−Cl(1) = 78.1(2), Cl(4)−Zr(1)−Cl(1) = 94.93(9), C(51)−Zr(1)−Cl(3) = 76.2(2), Cl(4)−Zr(1)−Cl(3) = 86.28(8), Cl(1)−Zr(1)−Cl(3) = 153.58(8), C(51)−Zr(1)−Cl(2) = 75.1(2), Cl(4)−Zr(1)−Cl(2) = 154.22(8), Cl(1)−Zr(1)−Cl(2) = 82.87(9), Cl(3)−Zr(1)−Cl(2) = 84.72(8), C(53)−Zr(2)−C(51) = 74.9(3), Cl(5)−Zr(2)−Cl(2) = 149.56(8), C(53)−Zr(2)−Cl(1) 147.9(3), C(51)−Zr(2)−Cl(1) = 73.1(2), Cl(2)−Zr(2)−Cl(1) = 77.73(8), C(52)−Zr(3)−C(51) = 74.8(3), C(52)−Zr(3)−Cl(6) = 90.4(2), C(51)−Zr(3)−Cl(6) = 79.2(2), C(52)−Zr(3)−Cl(4) = 147.9(2), C(51)−Zr(3)−Cl(4) = 73.1(2), Cl(6)−Zr(3)−Cl(4) = 84.55(8), C(52)−Zr(3)−Cl(3) = 91.3(2), C(51)−Zr(3)−Cl(3) = 71.9(2), Cl(6)−Zr(3)−Cl(3) = 149.53(8), Cl(4)−Zr(3)−Cl(3) = 78.07(8), C(52)−Zr(4)−C(53) = 92.3(3), C(52)−Zr(4)−C(51) = 75.3(3), C(53)−Zr(4)−C(51) = 75.2(3), C(52)−Zr(4)−Cl(3) = 87.7(2), C(53)−Zr(4)−Cl(3) = 145.6(3), C(51)−Zr(4)−Cl(3) = 71.5(2), C(52)−Zr(4)−Cl(2) = 145.0(3), C(53)−Zr(4)−Cl(2) = 85.3(2), C(51)−Zr(4)−Cl(2) = 70.3(2), Cl(3)−Zr(4)−Cl(2) = 75.53(7), C(52)−Zr(5)−C(53) = 88.8(3), C(52)−Zr(5)−C(51) = 70.0(3), C(53)−Zr(5)−C(51) = 70.1(3), C(52)−Zr(5)−Cl(5) = 144.1(3), C(53)−Zr(5)−Cl(5) = 84.5(2), C(51)−Zr(5)−Cl(5) = 74.6(2), C(52)−Zr(5)−Cl(6) = 83.8(2), C(53)−Zr(5)−Cl(6) = 144.0(3), C(51)−Zr(5)−Cl(6) = 74.3(2), Cl(5)−Zr(5)−Cl(6) = 81.28(8), Zr(4)−C(51)−Zr(1) = 103.6(3), Zr(4)−C(51)−Zr(2) = 88.4(3), Zr(1)−C(51)−Zr(2) = 97.3(3), Zr(4)−C(51)−Zr(3) = 87.2(3), Zr(1)−C(51)−Zr(3) = 96.2(3), Zr(2)−C(51)−Zr(3) = 166.4(4), Zr(4)−C(51)−Zr(5) = 79.5(3), Zr(1)−C(51)−Zr(5) = 176.9(5), Zr(2)−C(51)−Zr(5) = 83.5(3), Zr(3)−C(51)−Zr(5) = 83.0(3), Zr(3)−C(52)−Zr(4) = 95.8(4), Zr(3)−C(52)−Zr(5) = 94.3(4), Zr(4)−C(52)−Zr(5) = 86.4(3), Zr(2)−C(53)−Zr(4) = 95.7(4), Zr(2)−C(53)−Zr(5) = 93.7(4), Zr(4)−C(53)−Zr(5) = 85.2(3).

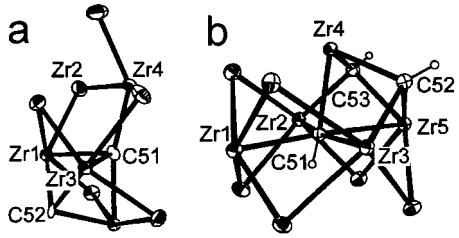

Figure 11. ORTEP drawings of the Zr−C−Cl cores of compounds (a) **21** and (b) **22**.

the remaining Zr−C−Zr angles range from 86.4(6) to 104.6(8)° (Figure 11a).

A similar reaction of **3** with neat $AlMe_3$ in benzene afforded a similar mixture of reaction products as judged by ^{31}P NMR spectroscopy. One of these species crystallized from solution. The product **22** exhibits two ^1H methine resonances at 14.44 and 9.34 ppm in a ratio of 2:1, as well as four resonances attributable to pentamethylcyclopentadienyl methyl groups in a ratio of 1:1:2:1. $^1H-^{13}C$ 2D spectra confirmed the correlation of the ^1H resonances at 14.44 and 9.34 ppm with the ^{13}C resonances at 372.9 and 168.3 ppm, respectively. X-ray crystallography confirmed the formulation of **22** as $(Cp^*Zr)_5(\mu\text{-}Cl)_6(\mu\text{-}CH)_3$ (Figure 10). This species, like **21**, is a Zr cluster. Compound **22** is comprised of five Cp*Zr fragments about a central methine carbon atom. The Zr atoms form a square-based pyramid about the central carbon (C(51)), and the basal Zr atoms are bridged by four chloride atoms below the plane. Two chlorine atoms and two pseudo-tetrahedral methine carbons above the plane bridge the axial Zr center. Bridging Zr−Cl distances are similar to those seen in **21**, ranging from 2.507(3) to 2.774(2) Å for the basal Zr atoms and average 2.890(4) Å for the axial Zr atom. The geometries about the triply bridging methine carbons in **22** are similar to that seen in **21**. The geometry about the central carbon is that of a distorted octahedron (Figure 11b), with Zr−C distances ranging from 2.324(10) to 2.412(9) Å. The coplanar Zr atoms adopt a pseudo-square-planar arrangement about the C with Zr(2)−C(51)−Zr(3) and Zr(1)−C(51)−Zr(5) angles of 166.4(4) and 176.9(5)°, respectively. Zr(4) is approximately orthogonal to these Zr atoms, with Zr−C−Zr angles from 83.0(3) to 103.6(3)°. The located and refined hydrogen atom occupies the axial position approximately trans to Zr(4) (H−C−Zr = 174.4°). The distortion in the geometry about the central carbon is presumably a ramification of the molecular dissymmetry and the steric crowding of five Cp*Zr fragments. It is noteworthy that the related C−H bond activation products $[(Cp^*Zr)_3Al_6Me_8(CH_2)_2(CH)_4(CH)]$, $\{[(C_5Me_4Et)Zr]_3Al_6Me_8(CH_2)_2(CH)_4(CH)\}$, and $[(Cp^*Hf)_3Al_6Me_8(CH_2)_2(CH)_4(CH)]$ have been isolated in low yield by Roesky et al. from the reactions of $Cp'ZrF_3$ with varying equivalents of $AlMe_3$.[32,33]

The compounds **21** and **22** were obtained in poor yield from the reactions of **3** with $AlMe_3$, and thus it cannot be assumed that these products represent the major reaction pathways. Nonetheless, these compounds do suggest avenues by which catalyst−cocatalyst interac-

(32) Herzog, A.; Roesky, H. W.; Jager, F.; Steiner, A.; Noltemeyer, M. *Organometallics* **1996**, *15*, 909−917.
(33) Herzog, A.; Roesky, H. W.; Zak, Z.; Noltemeyer, M. *Angew. Chem., Int. Ed. Engl.* **1994**, *33*, 967−968.

tions can lead to deactivation. First, phosphinimide ligand abstraction clearly occurs in the formation of **21** and **22**, and thus this may also occur upon reaction of Zr−phosphinimide complexes with Al-based cocatalysts. This stands in contrast to the related Ti complexes, where phosphinimide ligands have been shown to bridge Ti and Al centers.[7,10] Second, methyl transfer from Al to Zr followed by C−H bond activation is clearly indicated by the isolation of **22** and **23**. Thus, C−H bond activation could be one route for catalyst deactivation. Recent studies of Ti−Al−carbide species derived from Ti−phosphinimide complex reactions with $AlMe_3$ suggest a similar proposition.[7,10]

Acknowledgment. Financial support from the NSERC of Canada and NOVA Chemicals Corp. is gratefully acknowledged.

Supporting Information Available: Figures giving NMR data and electronic files giving crystallographic data, in CIF format. This material is available free of charge via the Internet at http://pubs.acs.org.

OM010433Q